6 August 1965, Volume 149, Number 3684 SCIENCE

Field Ion Microscopy

Unique magnification and resolution reveal location of atoms on the surface of a variety of metals.

Erwin W. Müller

The physical properties of metals are profoundly influenced by lattice imperfections, some of which are beyond the range of the electron microscope. The field ion microscope (*1*) is a more powerful instrument, capable of showing directly the atoms of the specimen. It has been known for a number of years and is now coming into use as a tool for materials research (*2*). The slow acceptance of the instrument is probably due to the inherent limitations and difficulties of its operation. In the conventional optical or electron microscope the imaging process interacts very little with the specimen, as there are independent lenses and illuminating beams. In the field ion microscope the specimen itself is also the image-forming "lens," and the imaging ion beams originate at the specimen surface. Thus the image formation is intimately connected with the details of the atomic structures we want to observe. The proper use of the microscope and a successful image interpretation require the consideration of several physical effects which are only now becoming gradually understood, since they occur under most unusual conditions. Progress in field ion microscopy is determined by advances in the basic knowledge of physical processes at surfaces under extremely high electric fields, in the range of 500 million volts per centimeter.

The author is Research Professor of Physics at the Pennsylvania State University, University Park.

Principle of the Field Ion Microscope

The microscope displays the hemispherical surface of a needle-shaped specimen on a fluorescent screen. Originally, the image was formed by radial projection of field-emitted electrons (*3*); this results in a magnification equal to the ratio of screen distance to needle-tip radius. By proper etching of fine wires, needle tips having a radius of curvature of well below 1000 angstroms can be prepared, so that, with a typical tip-to-screen distance of 10 centimeters, magnification of more than 1 million is achieved. When field-emitted electrons are used for imaging, their tangential-velocity component (due to the large Fermi energy of metal electrons) and also the diffraction effect caused by their relatively long de Broglie wavelength limit the sharpness of the projected image to a resolution of about 20 angstroms. A decisive advance was made when the tip surface was imaged with ions of hydrogen or helium (*4*). The disturbing tangential-velocity component is reduced by cooling the emitter, while the diffraction effect becomes negligible because of the much shorter de Broglie wavelength. The potential resolution is approximately

$$\delta = \sqrt{\frac{6 \cdot 10^6 Tr}{F}} \text{ Å} \qquad (1)$$

where T is the tip temperature, in degrees Kelvin; r is the tip radius, in centimeters; and F is the field strength, in megavolts per centimeter. Actually, the experimentally observed resolution does not quite go down to this small dimension because of the finite ion diameter and the fact that ionization occurs within a certain distance above the surface. Adjacent atoms of a silicon crystal, 2.3 angstroms apart, have been separated occasionally, but the spacing between neighboring platinum or tungsten atoms—2.78 and 2.74 angstroms, respectively—can be more easily resolved.

The field ion microscope (Fig. 1) is operated with a gas filling, usually helium, at a pressure of 1 to 3 $\times$ 10^{-3} torr. Neutral gas molecules arrive at the tip at a rate 10 to 100 times greater than is expected on the basis of simple gas kinetics, because of the attraction of induced dipoles (*4*) in the inhomogeneous field near the tip. Upon collision with the tip surface, the gas molecules transfer some of their kinetic energy to the lattice. As a result, their rebound energy may be too small to let them escape from the high field region around the tip. Trapped by dipole attraction but not permanently adsorbed, they "hop" (*5*) over the tip surface until, after having been slowed down in a sequence of up to several hundred contacts, they lose one electron by tunneling (Fig. 2). This is most likely to happen in the locally enhanced field above a protruding surface atom, and it is possible only beyond a certain minimum distance where the ground level of the electron in the helium atom lies above the Fermi level in the metal (*6*) (Fig. 3). A striking result of recent measurements of the energy distribution of these ions (*7*) is the finding that they originate almost entirely within disk-shaped zones that float above the atoms of the tip surface. Each of these disk-shaped zones, represented schematically by the dashes above the atoms in Fig. 2, has a depth of less than 0.2 angstrom and a radius of about 1.5 angstroms. It is separated from the electronic surface of the corresponding atom by a distance of 4 angstroms. The ion formed within this zone is accelerated by the field and travels in a radial direction toward the

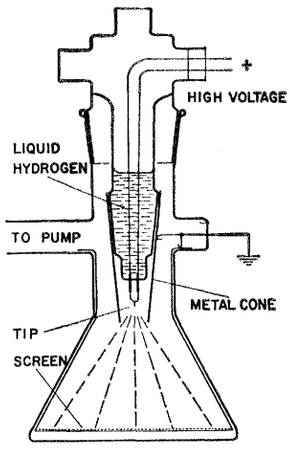

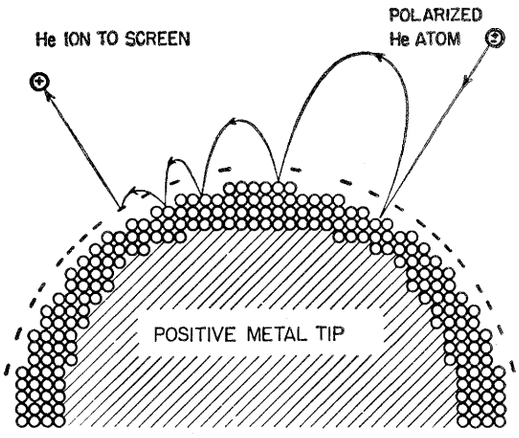

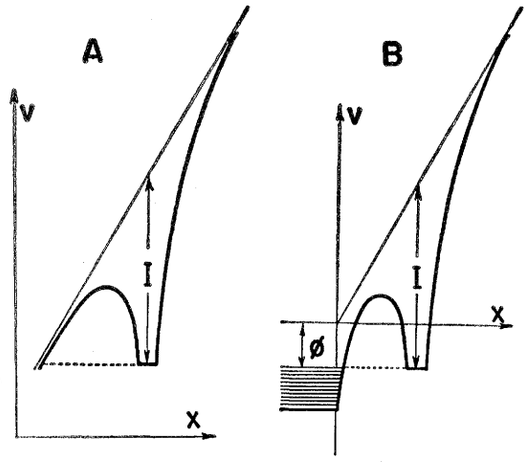

Fig. 1 (left). Schematic drawing of a field ion microscope. Fig. 2 (center). A polarized helium atom is attracted to the metal tip, is slowed down in a number of hops, and is ionized in the ionization zone (0.2 Å thick) over a protruding atom. The helium ion is accelerated toward the screen (see Fig. 1). Fig. 3 (right). (*A*) The potential funnel of an atom in a strong electric field; (*B*) the potential of an electron near the metal surface. Field ionization of the gas atom occurs when the electron from the ground state tunnels along the dotted line into the metal to the left.

screen. Under typical operating conditions, individual atoms of the metal surface produce some 10^4 to 10^6 ions per second, depending upon the degree of protrusion, which gives clearly visible image dots on the screen. A tip of 1000-angstrom radius has some 10^5 surface atoms protruding sufficiently to cause localized ionization, so that the total ion image consists of some 10^{10} ions per second, or an ion current in the 10^{-9}-ampere range. This is a fairly weak image that requires perfect dark adaptation for visual observation, large-aperture optics with about a minute of exposure time for photographic recording, and electronic image amplification for motion-picture photography.

Imaging by radial projection depends critically upon the ability to produce a nearly hemispherical, atomically smooth specimen surface. Chemical etching and electropolishing of a fine wire is the first crude step. The finish to the almost incredible perfection exemplified by the platinum crystal hemisphere in the cover photograph, with its more than 1000 crystal facets of highest atomic regularity and almost absolute purity, can only be achieved by an effect discovered only 10 years ago—field evaporation (*8*). Evaporation of solids or liquids commonly occurs when thermal activation permits surface atoms to overcome the potential barrier presented by the sublimation energy Λ. However, when a sufficiently high electric field is applied, surface atoms may also be removed as ions when they leave one or two of their electrons behind. For the purpose of tip polishing this effect is ideally self-regulating, since the local field enhancement at sharp edges and protrusions causes these to evaporate preferentially. This process can be carried out inside the field ion microscope and at any desired low temperature. The evaporation field is reached when the electric force acting on the metal ion, plus a small thermal activation energy, overcomes the binding energy, to which a polarization term has to be added. The image force theory of field evaporation (*8, 9*) leads to the equation

$$F = n^{-3}\, e^{-3} \times \left[\Lambda + I_n - n\phi + \tfrac{1}{2}(\alpha_o - \alpha_i)\, F^2 - kT \ln \frac{t}{t_o}\right]^2 \quad (2)$$

where F = field strength for evaporation; ne = single or multiple electric charge of the ion (n = 1 or 2); $\Lambda \simeq$ vaporization energy of the metal atom; I_n = its nth ionization energy; ϕ = work function of the specific crystal plane; α_o = polarizability of the metal atom at the surface site; α_i = polarizability of the free metal ion; k = Boltzmann's constant; T = absolute temperature; t = time required for evaporation; and t_o = vibration time of the bound surface atom.

Unfortunately it is not possible to accurately calculate the expected evaporation field because, for several metals, the second ionization potentials, I_2, are not well known. The same is true for the work function, which varies by more than 1 electron volt at certain crystal planes of a metal, and there are various ways (*10, 11*) to arrive at a reasonable figure for α_o. As a first approximation, a value of 1 electron volt has been taken here as the polarization

Table 1. Evaporation fields (F), in megavolts per centimeter, for singly and doubly charged metal ions.

Metal	F^+	F^{++}
W	1190	530
Re	980	460
Ta	1100	450
Mo	795	388
Nb	800	342
Ir	955	541
Pt	761	488
Zr	700	345
Au	570	505
Fe	490	352
Ni	445	385
Cu	410	475
Zn	383	388

Table 2. Data on field ion microscopy with various gases.

Gas	I (electron volts)	Image field (Mv/cm)	Practical temperature (deg K)	Potential resolution for 500-Å tip radius (Å)
He	24.6	450	20	1.2
Ne	21.6	370	20	1.3
H_2	15.6	228	20	1.6
A	15.7	230	80	3.2
Kr	14.0	194	80	3.5
Xe	12.1	156	80	4.0
N_2	15.5	226	80	3.3
O_2	12.5	164	80	3.8
Hg	10.4	124	300	8.5
Cs	3.9	28	400	21.0

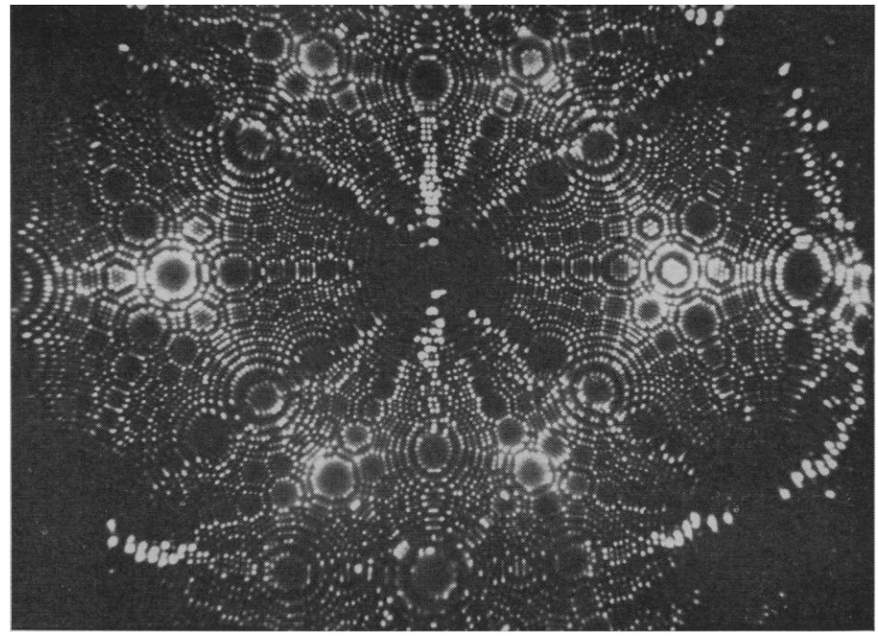

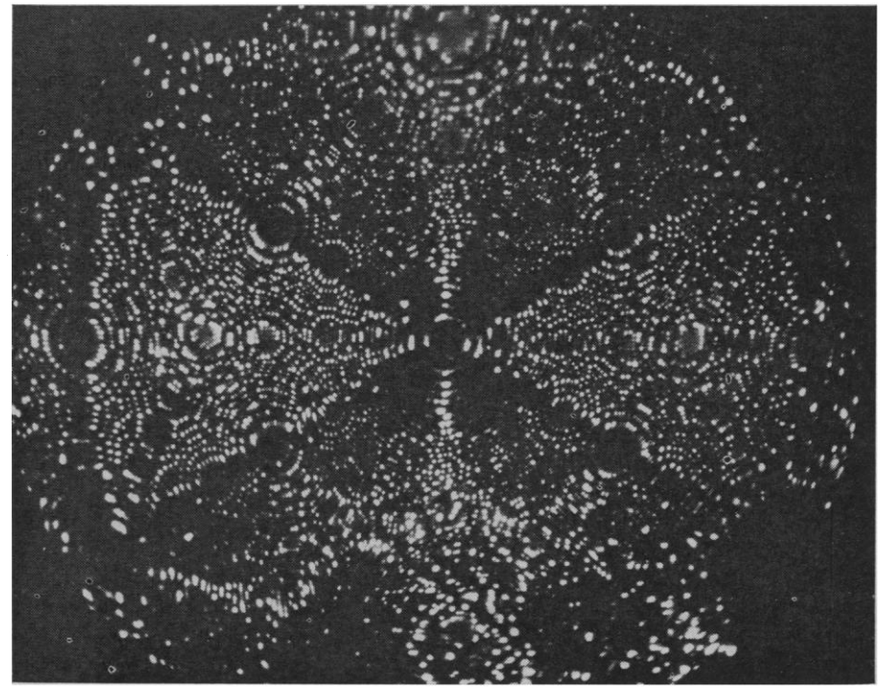

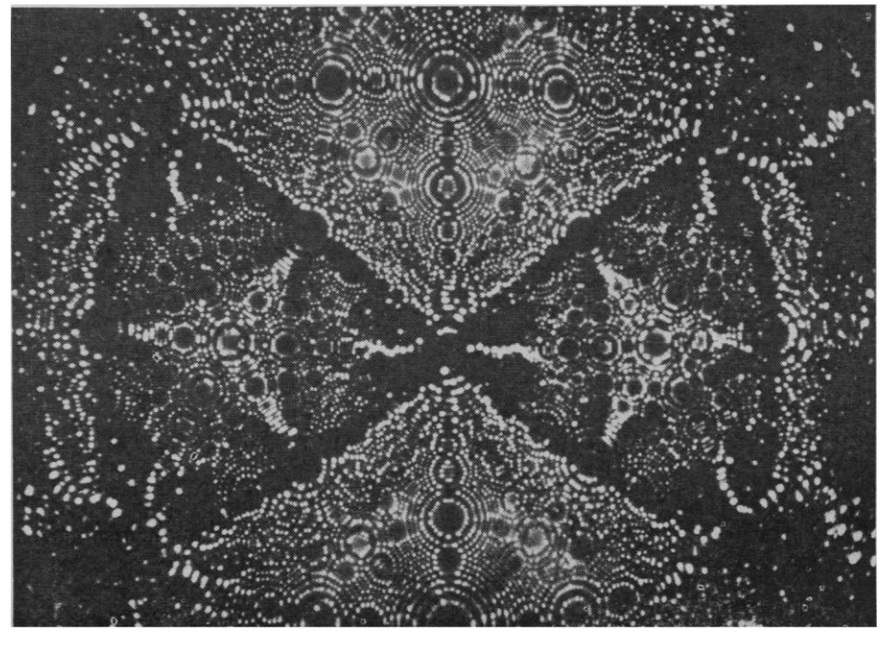

Fig. 4 (top). Field-evaporation end form of a tungsten crystal of approximately 600-Å radius. Fig. 5 (middle). Field-evaporated molybdenum tip of about 750-Å radius. Fig. 6 (bottom). Field-evaporation end form of a tantalum tip of approximately 800-Å radius. All three crystals (Figs. 4–6) have a body-centered cubic lattice, and are shown in the same orientation, with the (011) plane in the center, the cube planes below and above, and the triangular {111} regions to the left and the right.

binding energy at the evaporation field for all metals. Table 1 lists the resulting calculated evaporation fields at $T = 0°K$ for the metals most commonly used in field ion microscopy. According to this table, all the metals listed except copper and zinc should be doubly charged when field evaporation occurs; the observed magnitude of the evaporation field agrees quite well with this prediction, which was first made by Brandon (*11*). Indeed, tungsten has been observed with a mass spectroscope to evaporate as W^{++} (*1*), and copper, as Cu^{+} (*12*).

A tip does not evaporate to an exact hemisphere. Since all atoms which are exposed to too high a field because of their protruding position are removed, the end form of a tip of isotropic material would be an oblate hemispheroid characterized by a uniform field strength all over the surface except for a transient region toward the shank where F drops quite suddenly. The oblate hemispheroid shape is further modified by the variations of the work function ϕ and the polarizability α_n with crystallographic orientation. As may be seen from Eq. 2, removal of exposed atoms in areas of low work function or of high polarizability requires a higher field strength; in the field-evaporation end form, these areas should have a relatively small local radius of curvature. This expectation is confirmed by experiment. Local radii of curvature of tip areas can be accurately measured by counting the number of net plane rings between a set of crystal planes of known orientation. The net plane rings represent a kind of topographic map of the surface, with the net plane spacing determining the steps in elevation. At present, work functions of different crystal planes are fairly accurately known for only one metal (tungsten), and surface polarizabilities, for none. The distinct differences between the field-evaporation end

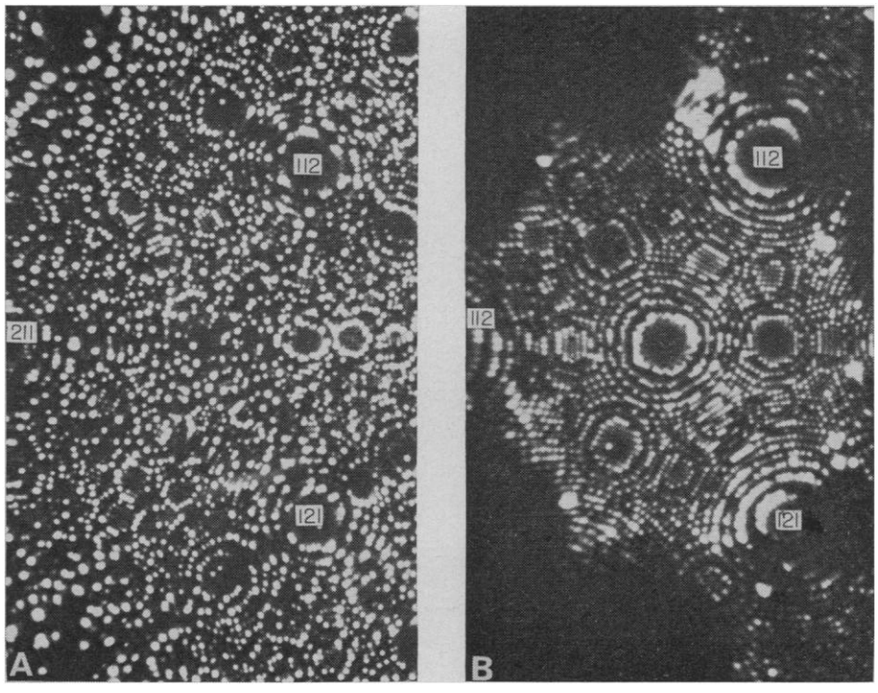

Fig. 7. Helium ion image of the (111) region (center) of a niobium tip. (*A*) Crystal field-evaporated at 21°K in helium, with many niobium atoms at metastable sites, appearing as extra-bright dots. (*B*) The same cystal field-evaporated and imaged at a reduced field in a He-D_2 mixture. A number of vacancies appear at various net planes.

form of the three refractory metals with body-centered cubic lattice—tungsten (Fig. 4), molybdenum (Fig. 5), and tantalum (Fig. 6)—might indeed be due to the specific electronic structures of the metal surfaces, but in the absence of data no quantitative predictions can be made.

There is also a difference in image intensity at various crystallographic regions of the three metals which cannot be accounted for by local field variations due to differences in radius of curvature. The assumption of a fairly large crystal orientation and material-dependent reflection coefficient for an electron about to tunnel out of an imaging gas atom could best explain the obvious differences in probability of ionization above various crystal planes.

Various Imaging Gases

The onset of field evaporation limits the field that can be applied for imaging. When observed at liquid-hydrogen temperature, tungsten, rhenium, iridium, platinum, molybdenum, tantalum, niobium, and rhodium are stable at the approximately 450 megavolts per centimeter required for helium ionization, while zirconium, vanadium, palladium, titanium, nickel, and iron are quite marginal. There are two obvious means of extending field ion microscopy to these latter materials, and to others in which field evaporation occurs at even lower fields. One is the use of gases with lower ionization potentials, I, to obtain images at correspondingly lower fields. The other is the use of image intensification in order to cut down the exposure time for photographing a continuously evaporating specimen surface. The tunneling mechanism for ionization suggests that the image fields (*1*) are approximately

$$F = 3.7 \cdot I^{3/2} \qquad (3)$$

(F is in megavolts per centimeter when I is measured in electron volts); values for a number of imaging gases are listed in Table 2.

Unfortunately, there are various difficulties connected with the use of gases of lower ionization potential. Only for helium, neon, and H_2 can liquid-hydrogen cooling be used, while the other gases and vapors require higher operation temperatures because of condensation. The actually obtainable resolutions may be considerably less than the potential resolution because of the finite diameter of the imaging ions and the location of their origin somewhat away from the surface. Very promising results have recently been obtained with neon (*13*); with neon, all the metals listed in Table 1 can be imaged below or at their evaporation field. Helium and neon both have much higher ionization potentials than the impurity gases of a vacuum system, and not even one contaminating gas molecule can approach the freshly field-evaporated, and therefore atomically clean, metal surface as long as the field is not reduced to below about 350 Mv/cm. It is this feature of field ion microscopy that made it possible to use conveniently demountable, unbaked vacuum systems without sacrificing absolute atomic-surface cleanliness (*14*). This, from the practical point of view, very significant advantage is given up when gases of low ionization potential are used for imaging. Use of hydrogen, argon, or certain other gases requires a microscope tube that can be proc-

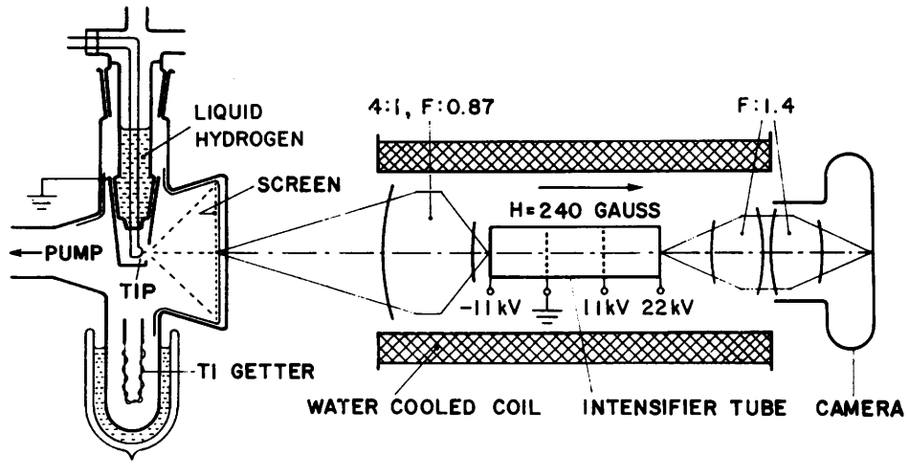

Fig. 8. Schematic diagram of a field ion microscope with external image intensifier.

essed for ultrahigh-vacuum cleanliness before admission of the purified imaging gas (*15*). There seems to be another serious disadvantage in the use of low ionization potential gases: their relatively large impact energy, $\frac{1}{2}\alpha F^2$, is effectively transferred to the surface and may disarrange the atomic structure (*13*).

The field required for the best image conditions is not a constant for each gas because the ionization probability depends upon the efficiency with which the field-trapped, hopping molecules are slowed down. The size of the tip radius (*16*) and, above all, the accommodation coefficient play a role. The energy transfer from a light helium atom to a heavy metal atom of the tip surface is extremely inefficient because of the great differences in masses of the collision partners; for tungsten the thermal accommodation coefficient of helium has been found to be as small as 0.015 and nearly independent of temperature down to 20°K (*17*). When as little as 5 percent of neon is added to the helium gas, the accommodation is much improved, the best image field is somewhat lowered, and the rendition of image details is much better. Even more effective is a trace of hydrogen or deuterium, which will form an invisible adsorption layer and, by acting as an intermediate collision partner, increase the accommodation coefficient of helium so much that a perfect helium ion image is obtained at 70 percent of the original field strength (*18*) (Fig. 7).

This little trick may well mean a breakthrough for field ion microscopy of the common transition metals, which previously could not be imaged very well with helium. In the actual performance of the experiment, the amount of hydrogen or deuterium to be added must be carefully controlled because these gases also promote field evaporation. While not much is gained as a useful margin between image field and evaporation field, with this method the specimen is subjected to less mechanical stress.

Image Intensification

A major problem in field ion microscopy is the low intensity of the image. No more ions can be drawn from the tip than are supplied to it as neutral gas molecules. The supply is proportional to the pressure, which in practice is limited to a few times 10^{-3} torr by the condition that the ions have to travel from the tip to the screen without being scattered by collisions. A dynamic gas supply system has been used (*19*) in which the tip is placed in a region of higher gas density near the center of a fine aperture, beyond which the gas is continuously being removed by a fast pump, so that the ion beam travels mostly in a region of low pressure with a long free path.

Attempts at image intensification by various means inside the ion microscope (*20*) have met with only limited

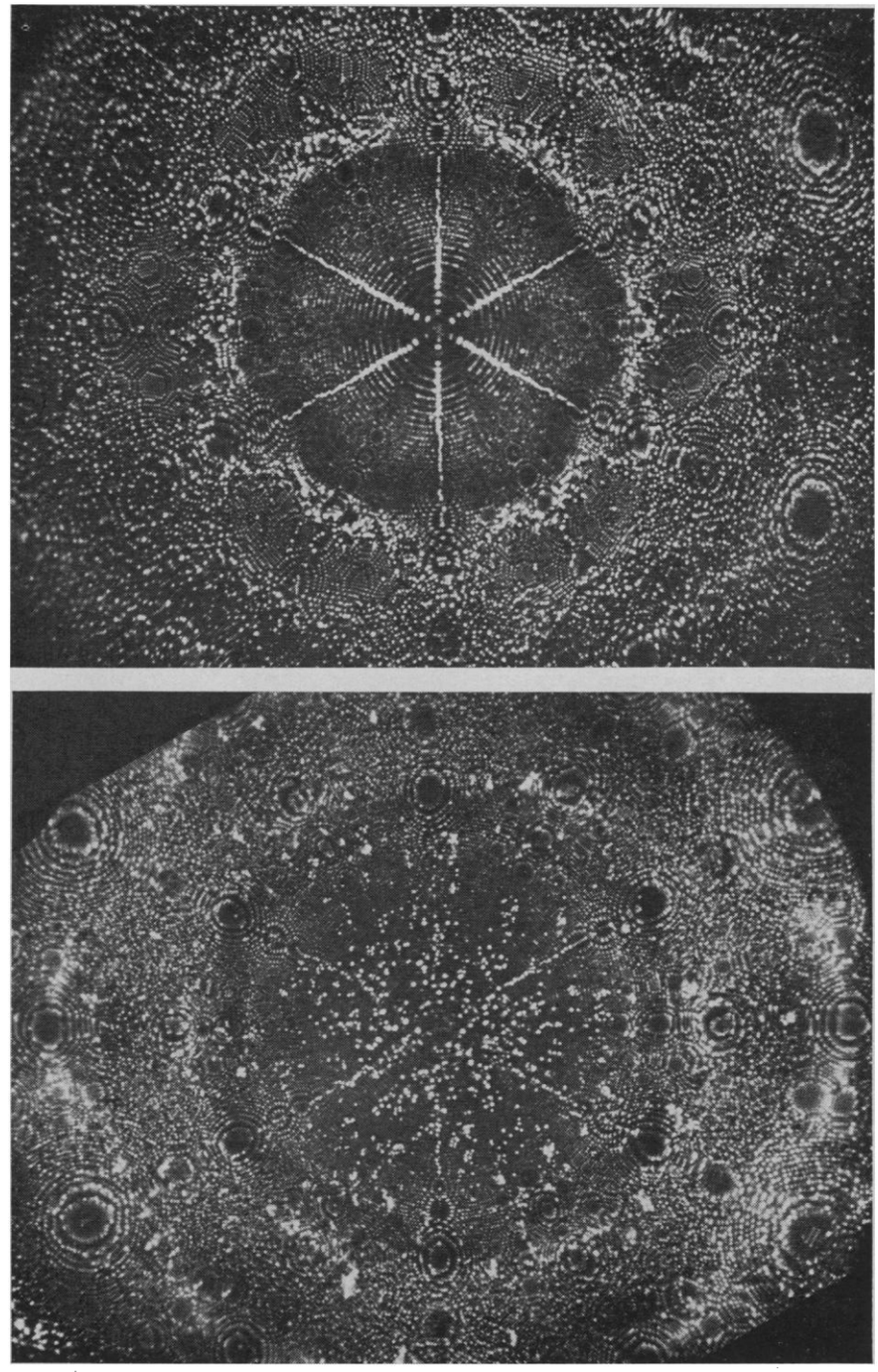

Fig. 9. (Top) Hexagonal rhenium crystal with the (0001) plane in the center. The six [2$\bar{1}\bar{1}$0]-zone lines are decorated by rows of bright atoms in field-stabilized sites. There is a crystallographically disturbed region about 25 degrees off the [0001] axis. (Bottom) The same rhenium tip after bombardment with radially impinging heavy negative ions of 27-kev energy. In the central region the damage appears only as individual bright spots, indicating the end of a collision sequence. In the disturbed region the damage forms large clusters or spikes.

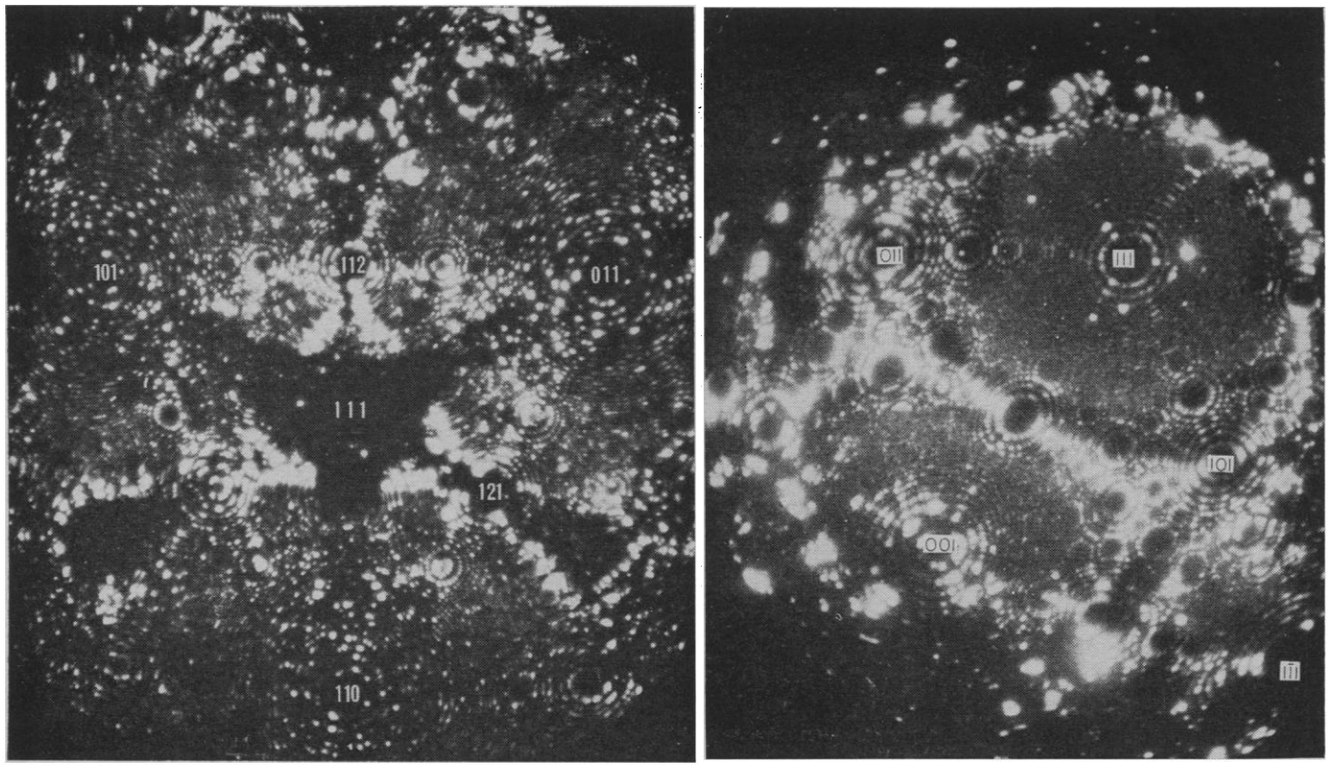

Fig. 10 (left). Iron tip imaged with helium, showing a depression in the (111) region caused by field-stress-induced lattice imperfections. Fig. 11 (right). Gold tip imaged with a helium-neon mixture at 17.6 kv, photographed with an image intensifier, with F:2.8 optics and 1/15-second exposure time.

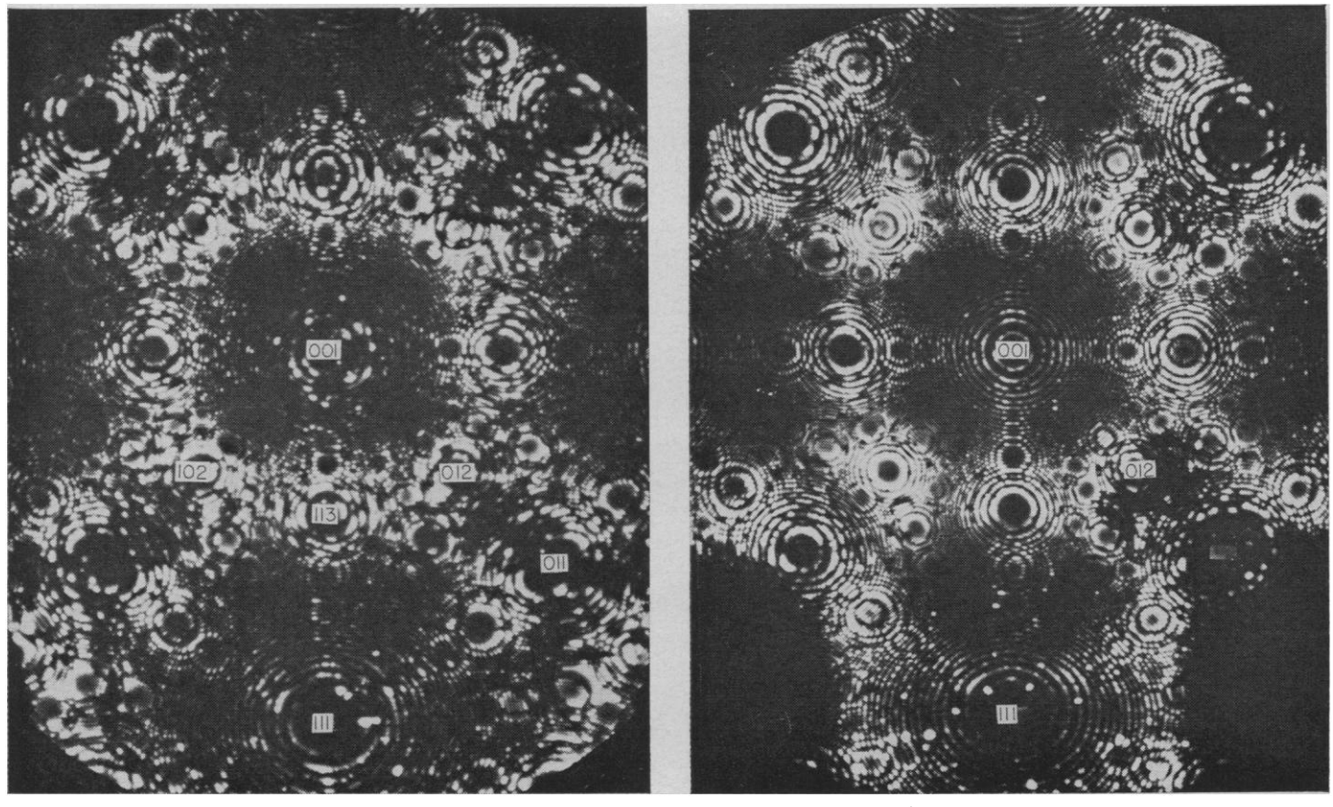

Fig. 12. (Left) Nickel tip imaged with helium. The field stress produces many dislocations in the 102–103 regions. (Right) Nickel tip imaged with helium after hydrogen-promoted field evaporation at a reduced field. The stress-sensitive regions are now nearly perfect.

success. A simple method is "post-acceleration" of the ion beams after passage through a fine, high-transmission wire mesh, but disturbing double images of ions and neutrals, produced by charge-exchange collisions, may occur. Moreover, postacceleration is only advisable for helium and hydrogen. For the heavier gases the screen efficiency is so low that even postacceleration to 50 kilovolts does not increase the image brightness very much, while at the same time the life of the screen is short. Conversion of the ion image into an electron image by using secondary electron emission from a fine grid is a somewhat more promising possibility for image intensification (*21*). An impressive intensification by a factor of 80 has been achieved for neon (*22*), but the onset of field emission from the grid and loss of resolution are serious limitations.

Recently developed external electronic image intensifiers based on photoelectric emission have proved to be most successful (*23*). A commercial three-stage RCA tube gave an overall gain of more than 10,000 at a low noise level (Fig. 8). Single-shot photographs of tungsten and platinum tips were obtained with exposure times down to 1/1000 second. Motion pictures have been made both in real time and in slow motion, since up to 64 frames per second could be photographed with helium and 16 frames per second with neon as the imaging gas. The intensifier, 3.8 centimeters (1½ inches) in diameter, is capable of resolving 400,000 image points, and with proper matching of optical magnification and field of view, closely packed net planes have been resolved. The noise in the tube is not disturbing at the image level used because the noise spots are easily distinguished from atom spots, both by their smaller size and by their short duration.

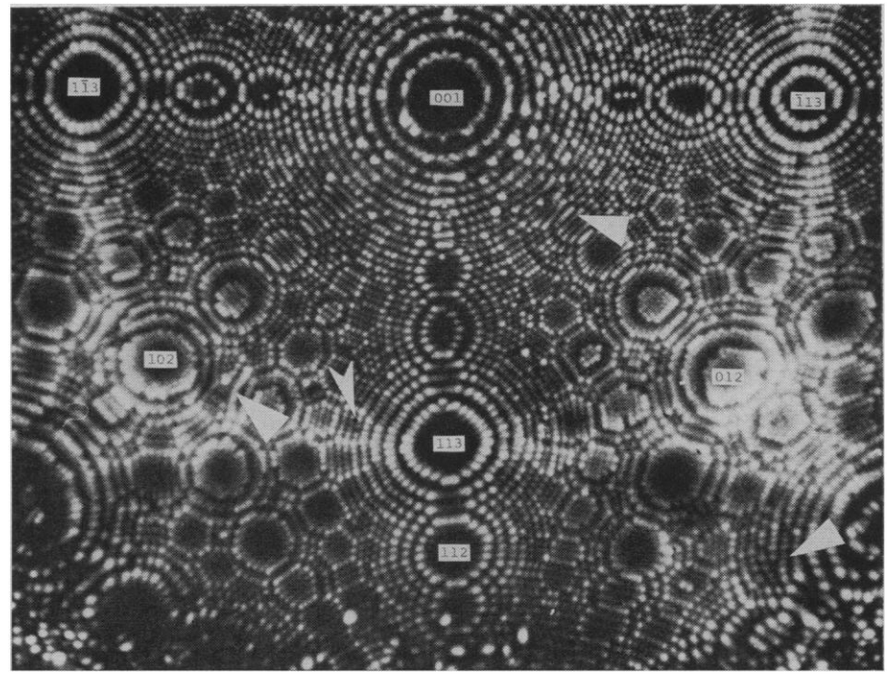

Fig. 13. Platinum crystal with a number of dislocations. The dislocation core near the (102) plane is decorated with an impurity atom, appearing as a bright spot. A vacancy is seen near the (113) plane.

Field-Induced Artifacts

The use of a well-designed image-intensification system is certainly most convenient in field ion microscopy of the common metals of fairly low melting point. The motion of net plane rings collapsing during field evaporation can now be stopped very near best-image conditions with single-shot photography, but neither such helium images nor the images obtained at considerably lower fields with neon are comparable in crystal perfection with those that can be obtained with the refractory metals. The nonrefractory metal specimens do not develop a high degree of crystal perfection when observed dynamically during field evaporation because the surface atoms do not evaporate in the proper sequence from the kink sites at dissolving net plane edges. At such a site on a body-centered cubic lattice the atom has four nearest neighbors, but when moved away by a short distance to a place where it has only three nearest neighbors (a "3-coordination site"), it might be more tightly bound by polarization because of increased exposure to the field. Deeper field penetration into such an atom at a low-coordination, metastable site also seems to increase the probability of ionization of the hopping imaging-gas molecules, so that the image of such an atom appears much brighter (*10*). The distinct decorations of the [001] zone of tungsten, the [110] zone of platinum, and the [$1\bar{1}21$] zone of rhenium (Fig. 9), to give an example for each of the simple lattice types, are explained as images of individual atoms at field-stabilized, low-coordination sites. Metastable sites also occur at other, rather restricted crystallographic areas of tungsten, in wider regions of tantalum, and almost everywhere when niobium is field-evaporated at 21°K (Fig. 7). The delicacy of balance between an ordinary 4-coordination kink site and a 3-coordination site with increased field-penetration binding is demonstrated by the temperature dependence of the field-evaporation end form of zone-refined tungsten. Field evaporation at 21°K always shows a number of bright, somewhat randomly arranged spots on the one side of the [$\bar{1}\bar{1}1$] zone line, particularly on the edges of the (112) and (123) planes, and covering the areas of the (225), (236), and (135) planes (Fig. 4). Also characteristic is a double edge on the side toward the cube planes of the (112) planes. These are all single tungsten atoms in field-stabilized 3-coordination sites. In contrast, field evaporation of the tip at 80°K develops absolutely perfect net plane edges in the same region. This striking effect of a higher surface lattice perfection at elevated temperature can also be observed on tantalum (*24*), with the difference that the field-stabilized "disorder" extends to a slightly larger area and that the perfect form requires field evaporation above 150°K. At that temperature tantalum also develops the [001] zone decoration and begins to resemble the familiar tungsten pattern.

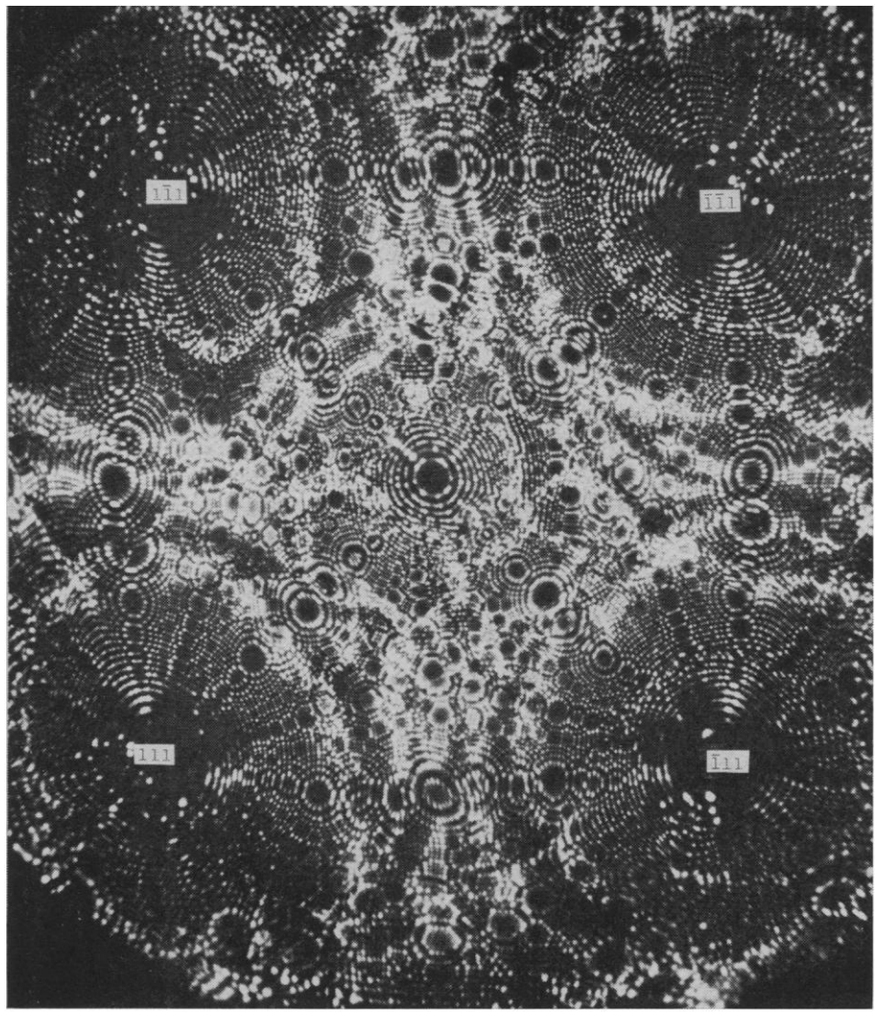

Fig. 14. Platinum crystal with slip bands concentric to the four {111} planes. The crystal was exposed to a field of 200 Mv/cm at a temperature of 450°C; nondestructive yield occurred.

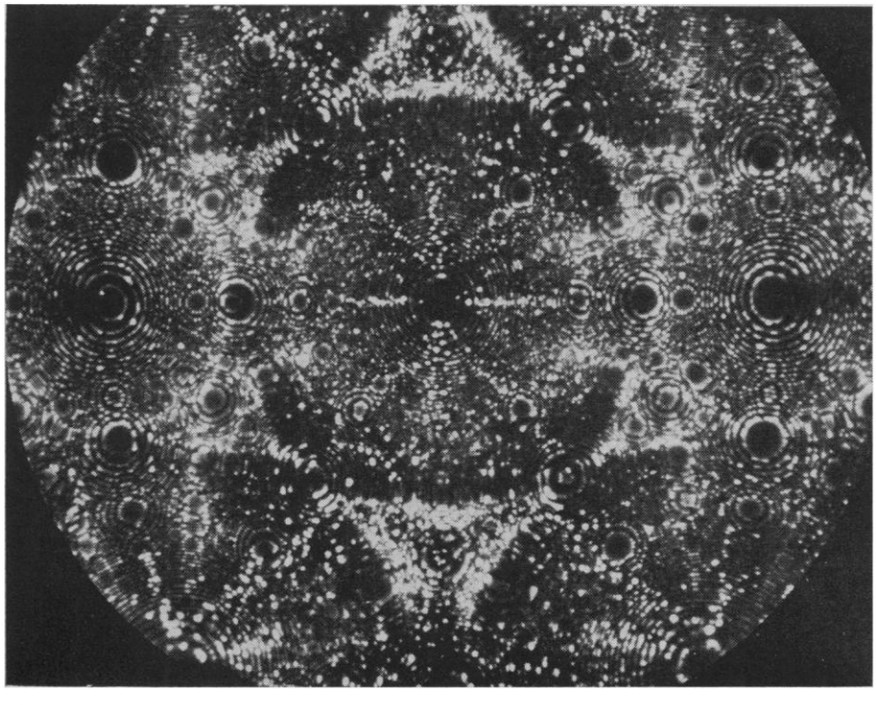

Fig. 15. Pure iron tip imaged with neon after hydrogen-promoted field evaporation. The tip radius is approximately 2000 Å.

Surface rearrangement to field-stabilized low-coordination sites becomes increasingly severe for some of the lower-melting materials. An extreme case is silicon, where the arrangement of atoms on the field-evaporated tip surface is almost completely random.

Besides the interaction between the field and the individual surface atoms, there is also a bulk effect. The mechanical stress exerted by an electric field on a conductive surface is

$$\sigma = F^2/8\pi \qquad (4)$$

(in dynes per square centimeter if F is measured in electrostatic units). This stress amounts, at 500 Mv/cm, to 1.1×10^{11} dyne/cm^2, or to about 1 ton/mm^2, often exceeding the technical yield strength of the tip materials by a factor of 50. The shear component of the stress, due to the nonsphericity of the specimen, may cause dislocations to move, sometimes until the tip fractures.

Yield in restricted areas under the field stress is typical for even the refractory molybdenum. A close network of dislocations emerges in the {111} regions, while other areas of the crystal hemisphere remain perfect (Fig. 5). It appears that only with a tip of very small radius, below 200 angstroms, is there insufficient room for the defects to grow. Niobium behaves very similarly, while tantalum and tungsten are strong enough not to yield at their respective evaporation fields. Of the other body-centered cubic metals, only iron has been investigated thoroughly. Reflecting the strong anisotropy of Young's modulus of iron, the (111) region, specifically, assumes a completely amorphous structure (Fig. 10). As the number of next-nearest atomic neighbors is diminished, field evaporation on the (111) region occurs so readily that a depression of the surface results, into which one can "look" only by using neon as the imaging gas. Of the metals with face-centered cubic lattice, iridium, platinum, rhodium, and, most surprisingly, also gold (Fig. 11) and perhaps copper do not yield under their evaporation field. Palladium and particularly nickel, on the other hand, develop dislocation networks in the {102}–{113} regions, while both the {001} and the {111} regions remain intact (Fig. 12, left and right).

It is doubtful whether the field-induced dislocation tangles grow from intrinsic defects. Rather, nucleation of dislocation loops seems to take place. The field stress may be considered a

negative hydrostatic pressure of approximately 100 kilobars at 500 Mv/cm. Under this condition the ordinary bulk modulus of the metal, as known from compression measurements, suggests a volume expansion of some 5 to 10 percent. Actually, the elastic bulk modulus at a large negative pressure, so far not accessible to measurement, must be even larger because of the asymmetry of the atomic potential function. Elastic volume expansions exceeding those connected with the thermal expansion to the melting point must occur, and spontaneous vacancy formation appears possible. Let us take, as an example, the volume V_a of a vacancy in platinum to be equal to the atomic volume 15.1×10^{-24} cm^3; the energy of increasing the volume of the tip is

$$pdV = F^2/8\pi \cdot V_a = 0.94 \text{ ev}$$

at the evaporation field of 475 Mv/cm. This energy is 20 percent less than the actual energy of formation of a vacancy as measured from quenching experiments or by direct counting of vacancies with the field ion microscope, so that in the case of platinum we are assured of the absence of artificial formation of vacancies by the evaporation-field stress. This is obviously not true for metals such as nickel or iron; but, unfortunately, for most metals neither the volume nor the energy of formation of a vacancy are known accurately enough to predict the maximum field stress that could be applied without vacancy formation and a subsequent collapse of vacancy disks to form dislocations.

As field ion microscopy depends critically upon the shaping of the specimen without the introduction of severe lattice imperfections, whether evaporation or yield occurs first when the field is raised determines whether or not a metal can be studied with this technique. Theoretical prediction is inaccurate because it requires the balancing of two effects for which present theories are not well enough developed. The discovery that hydrogen promotes field evaporation (*1*) opens a promising escape from the predicament brought about by field-induced artifacts. When field evaporation is carried out in the presence of hydrogen or deuterium, the required field is reduced by some 5 to 20 percent for most metals; thus, nearly perfect specimen surfaces can now be developed from several metals previously inaccessible to field ion microscopy (Fig. 12, right).

Application of Field Ion Microscopy

With the techniques now well established, and aware of the necessity of cautious interpretation of images, we can look forward to an increase in applications for basic research in surface physics and physical metallurgy. The considerable range of the exploratory investigations already performed gives us a fairly clear picture of the most promising lines of inquiry.

Somewhat neglected during the early development has been the capability of the field ion microscope in locating individual adsorbed atoms and molecules; this capability gives much needed information about the effect of special lattice sites and surface defects upon adsorption phenomena. Admission of a small amount of gas before the field is applied will allow adsorption to take place at the previously perfect specimen surface; the surface can be studied when the field is again applied. Some of the more strongly bound adsorbates will remain adsorbed in the high field and can be seen directly. A considerable amount of corrosion and rearrangement of metal atoms occurs with the adsorption and subsequent field desorption of oxygen on tungsten and platinum (*1*, *25*), and of water vapor (*1*), nitrogen, and carbon monoxide on these two metals and on iridium (*26*). Unfortunately, it is not always possible to distinguish an adsorbate atom from a displaced metal atom. A detailed examination of the behavior of adsorbed nitrogen, carbon monoxide, and hydrogen, with tungsten as the substrate, has been made (*27*). In a comprehensive review by Ehrlich (*28*), the results were compared on the same adsorption systems with findings through flash-filament and field-electron-microscope techniques. The general significance of adsorption studies with the field ion microscope is somewhat limited by polarization due to the high field. The imaging gas is found to reduce the stability of the adsorbate. Ehrlich (*29*), following a suggestion by R. D. Young, explains this as being due to bombardment with slow electrons from the ionization process; there is stronger evidence (*13*) that the dipole attraction energy of impinging imaging-gas molecules should be responsible.

A task that may overtax the capability of the field ion microscope is the visualization of basic biological molecules. When placed on a specimen tip, they will not stand the rupture of the field stress, and when we resort to some

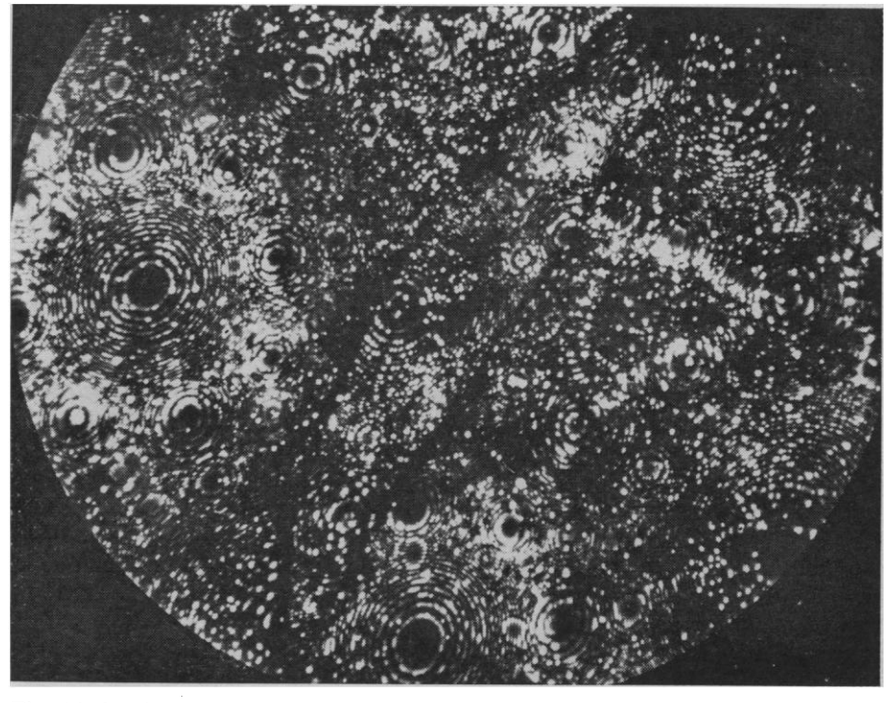

Fig. 16. Specimen of high-carbon steel, quenched from 900°C, annealed *in situ*, and imaged with helium after hydrogen-promoted field evaporation. A lens-shaped crystallite is formed between two grain boundaries. The three crystallites visible are all body-centered cubic. The many individual bright spots may be iron atoms stabilized in a protruding position by underlying carbon atoms.

kind of shadowing or imbedding with some sufficiently strong material, the promised high resolution will probably no longer be attainable.

The real strength of the field ion microscope lies in its ability to reveal the metal surface and to expose the bulk structure of the metal specimen by controlled layer-by-layer field evaporation. The atomic resolution is particularly useful for studying the bulk distribution of point defects. Vacancies were directly counted in platinum; the count revealed a density of 5.9×10^{-4} after quenching from near the melting point, a value which leads to the calculation of an energy of formation of 1.15 ev (*30*). In tungsten, however, no larger concentration than 10^{-4} was found, even after quenching from 3000°K at a rate of 450,000° per second. Vacancies and their clusters appear abundantly in α-particle or neutron-irradiated specimens of tungsten (*31*) and molybdenum (*32, 33*); the range of focusing collisions in such studies of radiation damage is clearly visible in ion micrographs. By preferred field evaporation of weakly bound substitutional impurity atoms or by corrosion through field-induced chemical reactions with strongly adsorbed oxygen, carbon monoxide, or nitrogen (*26*), surface vacancies which were originally not vacant lattice sites may be made to appear. The still-existing ambiguity in assigning the mobility observed in a narrow temperature range, during annealing of various bombardment-induced lattice defects to specific defects, can certainly be reduced through studies involving irradiation and annealing *in situ* in the field ion microscope.

The interpretation that the typical bright spots appearing upon *in situ* low-temperature irradiation with α-particles or fast helium atoms, or during cathode sputtering, represent interstitials lodged in subsurface sites is supported by the observation of bulk diffusion of such spots to the surface of irradiated tungsten by annealing in a narrow temperature range near 90°K (*34*). Distinct bright spots also indicate bulk impurity atoms such as oxygen in rhodium or in tantalum, or they may represent atoms or molecules of oxygen, nitrogen, or carbon monoxide adsorbed at the surface. Such spots are atomic surface sites having a sufficiently perturbed electric and geometric structure to modify, by increased field penetration, the local probability that the impinging gas will be ionized (*10*). Of the dislocations in a specimen, only those are visible that do not move out or multiply catastrophically under the field stress. The cores of edge and screw dislocations can be seen (Fig. 13), sometimes decorated by impurity atoms (*32*). Gradual field evaporation allows one to follow a single dislocation line or a complex grain boundary into the depth of the crystal (*35*) for many hundreds of atom layers. Slip bands (*14, 36*) can be produced *in situ* by pulling at the tip through application of a reduced electric field at elevated temperature (Fig. 14), and the growth of visible fatigue cracks has been caused by superimposing an alternating-voltage component to the tip voltage in order to cycle the stress (*37*). The considerable difference between the annealing end form and the field-evaporation end form of specimen tips was noted early (*1*), and rearrangement by annealing has been used to measure activation energies for surface migration on iridium (*38*).

Somewhat disappointing was the experience with solute alloys, which were found not to develop the desired surface perfection upon field evaporation because of the randomness of local binding energies (*33, 39, 40*). Interesting studies of impurity segregation, radiation damage, and slip behavior can be made, nevertheless; for dilute alloys, systems such as nickel-beryllium (1 percent) allow one to take a closer look at the process of precipitation. More rewarding is the investigation of ordered alloys, of which platinum (50 percent)-cobalt is the most easily studied (*39, 41*). Ordering and disordering of specimens can be carried out externally or *in situ*, and since the direction of the alternate layers of platinum and cobalt atoms can be seen, this material will be most useful in a variety of future experiments for elucidating such diverse problems as the effect of atomic size on field evaporation, the range and direction of focusing collisions resulting from radiation damage in layered media, the formation of vacancies and local stresses due to small deviations from stoichiometry, and the nucleation of ordering.

Most of the work so far has been done with the refractory metals, which, due to their strength, can stand the field stress most easily. It is now time to apply the advanced techniques that have been recently developed in this laboratory—such as image intensification, imaging with neon, and the promotion of field evaporation and ionization with hydrogen—to field ion microscopy of the common transition metals, the most challenging of which is iron or steel (Figs. 15 and 16). Field ion microscopy of refractory metals is basically a simple technique, and, with a small commercial instrument (*42*), a student can explore the atomic structure of tungsten in a 2-hour laboratory experiment. For more advanced original work with a wide variety of specimens, the equipment hardly need be more elaborate, except perhaps for the desirable provision of liquid-hydrogen or helium cooling. No high degree of mechanical perfection, such as is indispensable with the electron microscope, is required here. However, the experimentation becomes exceedingly delicate as one turns to the nonrefractory metals. Further advances in the exciting art of field ion microscopy will depend very little on instrumentation, but rather upon the skill, experience, patience, and ingenuity which the microscopist can muster for the preparation of the specimen, the making of the observation, and, finally, the interpretation of the image. It seems as if the evasive atoms still hide from the curious eye of the casual sightseer and reveal themselves rewardingly only to the serious researcher.

References and Notes

1. Basic developments of field ion microscopy are described in a review article: E. W. Müller, in *Advances in Electronics and Electron Physics*, vol. 13, L. Marton, Ed. (Academic Press, New York, 1960), pp. 83–179.
2. Field ion microscopy has been developed almost exclusively in the Field Emission Laboratory at the Pennsylvania State University, with gratefully acknowledged principal support over many years from the Air Force Office of Scientific Research, the Office of Naval Research, and the National Science Foundation. I thank my co-workers, particularly S. B. McLane, S. Nakamura, and O. Nishikawa, for their many contributions.
3. E. W. Müller, *Z. Physik* **106**, 541 (1937); the historical development of field emission research to 1956 is found in R. H. Good, Jr., and E. W. Müller, *Handbuch der Physik*, S. Flügge, Ed. (Springer, Berlin, 1956), vol. 21, p. 176.
4. E. W. Müller, *Z. Physik* **131**, 136 (1951).
5. ——— and K. Bahadur, *Phys. Rev.* **102**, 624 (1956).
6. A comprehensive account of the physical mechanism of field ionization is given by R. Gomer, *Field Emission and Field Ionization* (Harvard Univ. Press, Cambridge, 1961).
7. T. T. Tsong and E. W. Müller, *J. Chem. Phys.* **41**, 3279 (1964).
8. E. W. Müller, *Phys. Rev.* **102**, 618 (1956).
9. R. Gomer and L. W. Swanson, *J. Chem. Phys.* **38**, 1613 (1963).
10. E. W. Müller, *Surface Sci.* **2**, 484 (1964).
11. D. G. Brandon, *ibid.* **3**, 1 (1965).
12. E. W. Müller and R. Thomsen, unpublished.
13. O. Nishikawa and E. W. Müller, *J. Appl. Phys.* **35**, 2806 (1964).
14. E. W. Müller, in *Proc. Intern. Conf. Electron Microscopy, 4th, Berlin, 1958* (1960), vol. 1, p. 820.
15. ———, *Ann. Physik* **20**, 316 (1957).
16. ——— and R. D. Young, *J. Appl. Phys.* **32**, 2425 (1961).

17. L. B. Thomas and E. B. Schofield, *J. Chem. Phys.* **23**, 861 (1955); also a recent private communication.
18. E. W. Müller, S. Nakamura, S. B. McLane, *J. Appl. Phys.*, in press.
19. B. J. Waclawski and E. W. Müller, *ibid.* **32**, 1472 (1961).
20. D. G. Brandon, S. Ranganathan, D. S. Whitmell, *Brit. J. Appl. Phys.* **15**, 55 (1964).
21. M. von Ardenne, *Tabellen der Elektronenphysik I* (Deutscher Verlag, Berlin, 1956), p. 581.
22. D. G. Brandon, private communication.
23. S. B. McLane, E. W. Müller, O. Nishikawa, *Rev. Sci. Instr.* **35**, 1297 (1964).
24. S. Nakamura and E. W. Müller, *J. Appl. Phys.*, in press.
25. E. W. Müller, in *Structure and Properties of Thin Films*, C. A. Neugebauer, J. D. Newkirk, D. A. Vermilyea, Eds. (Wiley, New York, 1959), p. 476.
26. J. F. Mulson and E. W. Müller, *J. Chem. Phys.* **38**, 2615 (1963).
27. G. Ehrlich and F. G. Hudda, *ibid.* **36**, 3233 (1962).
28. G. Ehrlich, *Advan. Catalysis* **14**, 255 (1963).
29. ——— and F. G. Hudda, *Phil. Mag.* **8**, 1587 (1963).
30. E. W. Müller, *Z. Physik* **156**, 399 (1959).
31. ———, *Proc. Intern. Symp. Reactivity Solids, 4th, Amsterdam, 1960* (1961), p. 682.
32. ———, "Proc. Intern. Conf. Crystal Lattice Defects, Kyoto 1962," *J. Phys. Soc. Japan* **18**, suppl. II, 1 (1963).
33. D. G. Brandon, M. Wald, M. J. Southon, B. Ralph, *ibid.*, p. 324.
34. M. K. Sinha and E. W. Müller, *J. Appl. Phys.* **35**, 1256 (1964).
35. E. W. Müller, *Ann. N.Y. Acad. Sci.* **101**, 585 (1963); D. G. Brandon, B. Ralph, S. Ranganathan, M. S. Wald, *Acta Met.* **12**, 813 (1964).
36. E. W. Müller, *Acta Met.* **6**, 620 (1958).
37. ———, W. T. Pimbley, J. F. Mulson, in *Internal Stresses and Fatigue in Metals*, Rassweiler and Grube, Eds. (Elsevier, Amsterdam, 1959), p. 189.
38. S. S. Brenner, *Surface Sci.* **2**, 496 (1964).
39. E. W. Müller, *Bull. Am. Phys. Soc.* **7**, 27 (1962).
40. B. Ralph and D. G. Brandon, *Phil. Mag.* **8**, 919 (1963).
41. ———, *Proc. European Regional Conf. Electron Microscopy, 3rd, Prague, 1964* (1964), vol. 1.
42. The instrument is handled by the Central Scientific Company, Chicago 13, Ill.

But Is the Teacher Also a Citizen?

Alvin M. Weinberg

My subject is the connection between the university, particularly the scientific university, and society. Insofar as this connection affects the university's interests and its manner and style of teaching, I am concerned with the question, "But is the teacher also a citizen?" The tensions and contradictions I see in the relation between the modern scientific university and society are much the same as those described by others, but I describe them in a slightly different language, a language that comes from my own nonuniversity world.

Perhaps I should explain what this language is. I come from a large government laboratory. The laboratory is organized into 16 scientific divisions, each of which is concerned with a particular scientific discipline—that is, each is "discipline-oriented." But the primary purpose of the laboratory is to accomplish applied missions—desalting the sea economically, or providing an inexhaustible, cheap, energy source, or alleviating radiation disease. The laboratory as a whole is "mission-oriented." Thus our laboratory, like so many other institutions, has a dual structure—organizationally it is "discipline-oriented"; functionally it is "mission-oriented." To accomplish each mission we establish projects which cross divisional, disciplinary lines. A large project can involve a dozen divisions. This "mission-discipline duality" is evident in many social structures, not only in large laboratories. I see the relations between the university and society in terms of this duality.

The author is director of Oak Ridge National Laboratory, Oak Ridge, Tennessee. This article is based on a paper presented at the session "Whither the university?" of the Purdue University Symposium on Science and Public Policy, 14 April 1965, and as one of a series of lectures on College Teaching as a Career, Boston University, 15 April 1965.

The Mission-Discipline Duality

Our society is "mission-oriented." Its mission is resolution of problems arising from social, technical, and psychological conflicts and pressures. Since these problems are not generated within any single intellectual discipline, their resolution is not to be found within a single discipline. Society's standards of achievement are set pragmatically: what works is excellent, whether or not it falls into a neatly classified discipline. In society the nonspecialist and synthesizer is king.

The university by contrast is "discipline-oriented." Its viewpoint is the sum of the viewpoints of the separate, traditional disciplines that constitute it. The problems it deals with are, by and large, problems generated and solved within the disciplines themselves. Its standards of excellence are set by and within the disciplines. What deepens our understanding of a discipline is excellent. In the university the specialist and analyst is king.

The structure of the discipline-oriented university and the structure of the mission-oriented society tend to be incongruent. Moreover, as the disciplines making up the university become more complex and elaborate in response to their own internal logic, the discrepancy between the university and society grows. The university becomes more remote; its connection with society weakens; ultimately it could become irrelevant. The growth of this discrepancy appears to me to be a central problem in the relation between the university and society. It poses major difficulties for the university professor, especially in the natural sciences, who views his responsibility as a citizen broadly.

Harvey Brooks, dean of engineering and applied physics at Harvard University, put the matter with his usual incisiveness (*1*):

> The . . . issue is the relationship between science and technology in education. The original concept of an engineering school, as of a medical school, was an association of practitioners who used the benefit of their varied experience to teach young people. This tradition is somewhat maintained to this day in the field of architecture, but in both medicine and engineering the importance of the underlying sciences has become so great that medical and engineering faculties are increasingly populated with basic scientists who do research or teaching in sciences which are relevant to but by no means identical with the practice of medicine or engineering. The old form of teaching primarily by practicing physicians or engineers was found wanting because practical knowl-